

***Evaluation of Simplified Methods for Estimating Shear  
Capacity Using JNES/NUPEC Low-Rise Concrete Shear  
Wall Cyclic Test Data***

**Jinsuo Nie, Joseph I. Braverman, Charles H. Hofmayer, and Syed A. Ali\***

*Presented at the PVP 2008 Conference  
Chicago, Illinois, USA  
July 27-31, 2008*

**Energy Science and Technology  
Nuclear Energy and Infrastructure Systems Division/NE**

**(\* U.S. Nuclear Regulatory Commission)**

**Brookhaven National Laboratory  
P.O. Box 5000  
Upton, NY 11973-5000  
[www.bnl.gov](http://www.bnl.gov)**

Notice: This manuscript has been authored by employees of Brookhaven Science Associates, LLC under Contract No. DE-AC02-98CH10886 with the U.S. Department of Energy. The publisher by accepting the manuscript for publication acknowledges that the United States Government retains a non-exclusive, paid-up, irrevocable, world-wide license to publish or reproduce the published form of this manuscript, or allow others to do so, for United States Government purposes.

This preprint is intended for publication in a journal or proceedings. Since changes may be made before publication, it may not be cited or reproduced without the author's permission.

## **DISCLAIMER**

This report was prepared as an account of work sponsored by an agency of the United States Government. Neither the United States Government nor any agency thereof, nor any of their employees, nor any of their contractors, subcontractors, or their employees, makes any warranty, express or implied, or assumes any legal liability or responsibility for the accuracy, completeness, or any third party's use or the results of such use of any information, apparatus, product, or process disclosed, or represents that its use would not infringe privately owned rights. Reference herein to any specific commercial product, process, or service by trade name, trademark, manufacturer, or otherwise, does not necessarily constitute or imply its endorsement, recommendation, or favoring by the United States Government or any agency thereof or its contractors or subcontractors. The views and opinions of authors expressed herein do not necessarily state or reflect those of the United States Government or any agency thereof.



PVP2008- 61841

EVALUATION OF SIMPLIFIED METHODS FOR ESTIMATING SHEAR CAPACITY USING JNES/NUPEC  
LOW-RISE CONCRETE SHEAR WALL CYCLIC TEST DATA

Jinsuo Nie, Joseph I. Braverman, Charles H. Hofmayer  
Energy Science & Technology Department  
Brookhaven National Laboratory  
Upton, NY 11973-5000, USA  
Email: [jnie@bnl.gov](mailto:jnie@bnl.gov)

Syed A. Ali  
Division of Engineering  
Office of Nuclear Regulatory Research  
US Nuclear Regulatory Commission  
Washington, DC 20555-0001

**ABSTRACT**

The simplified methods in current codes for determining the shear capacity of reinforced concrete shear walls had mostly been validated using the test results of single-element shear walls. Recently available JNES/NUPEC test data of reinforced concrete shear walls under multi-directional cyclic loadings provided a unique opportunity to investigate the adequacy of the simplified methods for use in situations with strong interaction effects. A total of 11 test specimens with aspect ratios between 0.47 and 0.87 have been used in the assessment. Two simplified methods from the ACI 349-01 standard [1] and one from the ASCE 43-05 standard [2] have been evaluated. This paper also presents the development of an adjustment factor to consider the aspect ratio and the development of two approaches to consider interaction effects for one of the simplified methods. It concludes with the insights on the applicability of the code methods when interaction effects exist.

**INTRODUCTION**

Low-rise reinforced concrete shear walls are very common structural components in nuclear power plants (NPP) and have been designed with simplified methods prescribed by ACI codes in the U.S. These simplified methods have been primarily validated by the results of single-element shear wall

tests that included only the in-plane shear loading. Since NPP structures are commonly arranged in either box or circular shapes in plan and are subjected to bi-directional horizontal loadings (e.g. wind or seismic loads), the impact of the interaction of the bi-directional loadings on the ultimate shear capacity of the shear walls has not been specifically addressed by these simplified methods.

As part of collaborative efforts between the United States and Japan on seismic issues, the U.S. Nuclear Regulatory Commission (NRC) and Brookhaven National Laboratory (BNL) analyzed test data from a multi-year reinforced concrete shear wall test program conducted by the Japan Nuclear Energy Safety Organization (JNES) and Nuclear Power Engineering Corporation (NUPEC). The JNES/NUPEC shear wall tests included box-type and circular-type shear walls under multi-directional cyclic loadings and provided a unique opportunity to investigate the interaction effect and its implications on the simplified methods specified in design codes. A total of 11 tests of box-shaped shear walls with aspect ratios between 0.47 and 0.87 have been used in this evaluation.

The simplified methods prescribed by ACI codes have commonly been recognized as overly conservative, and have also been demonstrated to be quite conservative by recent BNL studies using the JNES/NUPEC test data. ASCE/SEI 43-05, a recently published standard entitled "Seismic Design Criteria for Structures, Systems, and Components in Nuclear Facilities," also presents a simplified method to compute the

DISCLAIMER NOTICE - The findings and opinions expressed in this paper are those of the authors, and do not necessarily reflect the views of the U.S. Nuclear Regulatory Commission or Brookhaven National Laboratory.

shear capacity of low-rise concrete shear walls. This method is reported to predict less conservative and more accurate shear capacity estimates than the ACI methods. These methods were evaluated in this study using the JNES/NUPEC test data to assess the accuracy of the methods when considering interaction effects.

This paper describes briefly the simplified methods, the relevant JNES/NUPEC tests, the comparison of the predicted results and the test data, and the insights gained from this study.

## CODE FORMULATIONS FOR SHEAR CAPACITY

Three simplified methods from ACI 349-01 and ASCE43-05 will be briefly overviewed in the following.

### ACI 349-01 Chapter 11 Method

Section 11.10 of ACI 349-01 under Chapter 11, "Shear and Torsion", prescribes the nominal shear strength  $V_n$  of reinforced concrete shear walls as a summation of the contribution from concrete  $V_c$  and the contribution from reinforcement  $V_s$ ,

$$V_n = V_c + V_s \quad (1)$$

$$V_c = 3.3\sqrt{f'_c}td + \frac{N_u d}{4l_w} \quad (2)$$

$$V_c = \left[ 0.6\sqrt{f'_c} + \frac{l_w \left( 1.25\sqrt{f'_c} + 0.2 \frac{N_u}{l_w t} \right)}{\frac{M_u}{V_u} - \frac{l_w}{2}} \right] td \quad (3)$$

$$V_s = \frac{A_v f_y d}{s_2} \quad (4)$$

$$V_n < 10\sqrt{f'_c}td \quad (5)$$

where  $V_c$  takes the smaller value of those obtained using Equations 2 and 3. The calculated shear strength from Equation 1 should be bounded by Equation 5. The parameters in the above equations are defined as,

- $f'_c$  = compressive strength of concrete
- $t$  = wall thickness
- $l_w$  = length of wall
- $d$  =  $0.8 \times l_w$ , per ACI 349-01, Section 11.10.4
- $N_u$  = factored axial load normal to cross section
- $M_u$  = factored moment at section
- $V_u$  = factored shear force at section
- $s_2$  = spacing of horizontal reinforcement
- $A_v$  = area of horizontal reinforcement within distance  $s_2$
- $f_y$  = yield strength of reinforcement

When expression  $\frac{M_u}{V_u} - \frac{l_w}{2}$  in Equation 3 is negative, then

Equation 3 shall not be used. Equation 2 determines the inclined cracking strength corresponding to a principal tensile stress of approximately  $4\sqrt{f'_c}$ ; while Equation 3 calculates the shear strength corresponding to a flexural tensile stress of  $6\sqrt{f'_c}$  at a section  $l_w/2$  above the section being investigated. Section 11.10 of ACI 349-01 specifies that the critical section to design for shear is from the base at a distance equal to one-half of the smaller of the wall length or the wall height.

The nominal strength calculation in this paper does not consider the strength reduction factor,  $\phi$  as described in the ACI code and in the ASCE 43-05 standard to be introduced, in order to obtain an estimate of the ultimate capacity rather than a design allowable value. Similar elimination of the strength reduction factor from the nominal strength calculation also applies to other methods in this paper for the same purpose.

### ACI 349-01 Chapter 21 Method

Section 21.6 of ACI 349-01 under Chapter 21, "Special Provisions for Seismic Design," provides requirements that apply to structural walls that are part of a seismic lateral load resisting system. Section 21.6.1 indicates that for shear walls with aspect ratio  $h_w/l_w$  of less than 2.0 ( $h_w$  is the height of the wall), the provisions in Section 21.6.5 for the shear strength can be waived. However, the nominal shear strength specified in this section will still be considered in this paper for purposes of comparison. For an  $h_w/l_w$  ratio less than 2.0, the nominal shear strength prescribed in this section can be determined by,

$$V_n = A_{cv} \left( \alpha_c \sqrt{f'_c} + \rho_n f_y \right) \quad (6)$$

$$V_n < 10A_{cv} \sqrt{f'_c} \quad (7)$$

in which parameters are defined as,

- $\alpha_c$  = 3 for  $h_w/l_w = 1.5$ ; 2.0 for  $h_w/l_w = 2.0$ ; and varies linearly in between
- $A_{cv}$  = the net cross-sectional area of a horizontal wall segment
- $\rho_n$  = the ratio of shear reinforcement on a plane perpendicular to plane of  $A_{cv}$
- $A_{cp}$  = the cross-sectional area of a horizontal wall segment;  $A_{cp}$  equals  $t \times l_w$  for a shear wall with solid cross section

### Comparison of ACI 349-01 Chapter 11 and 21 Methods

The differences in the ACI 349-01 Chapter 11 method and Chapter 21 method for nominal shear strength calculation for low rise shear walls ( $h_w/l_w < 2.0$ ) are tabulated below.

	Chapter 11	Chapter 21
1. Coefficient for $\sqrt{f'_c}$	3.3	2.0 to 3.0
2. Effect Length of wall $d$	$0.8 \times \text{length of wall}$	$1.0 \times \text{length of wall}$ (based on definition of $A_{cv}$ )
3. Comp. Load Contribution	$\frac{N_v d}{4l_w}$	None
4. Shear Upper Bound	$10\sqrt{f'_c}td$	$10A_{sp}\sqrt{f'_c}$

#### ASCE 43-05 Method

Barda, et al. [3] developed an empirical method to determine the ultimate shear strength of low rise reinforced concrete shear walls (aspect ratio  $h_w/l_w < 1.0$ ). In this method, the ultimate shear (stress) capacity  $v_u$  of the reinforced concrete shear wall is given by

$$v_u = v_{cu} + v_{su} \quad (8)$$

$$v_{su} = \rho_v f_y \quad (9)$$

$$v_{cu} = 8.3\sqrt{f'_c} - 3.4\sqrt{f'_c} \left( \frac{h_w}{l_w} - \frac{1}{2} \right) + \frac{N}{4l_w t} \quad (10)$$

where,

- $v_{cu}$  = shear (stress) capacity contribution from concrete
- $v_{su}$  = shear (stress) capacity contribution from steel reinforcement.
- $N$  = normal (bearing) load
- $\rho_v$  = vertical steel reinforcement ratio

A plot of the concrete strength versus aspect ratio for shear walls using the Barda equation is presented in Figure C4-1 of the ASCE 43-05 standard. Results from various tests are also shown on this plot for comparison. The test data points correspond only to the contribution of concrete (i.e., without the contribution from steel).

As indicated by Cover, et al. [4], the expressions given above for calculating the contribution of the steel reinforcement were modified to reflect the data of Shiga, et al. [5]; Cardenas, et al. [6]; and Oesterle, et al. [7]. The revised equation for  $v_{su}$  to consider the contribution of the horizontal and vertical steel reinforcement is given by,

$$v_{su} = (A\rho_v + B\rho_h) f_y \quad (11)$$

where,

- $\rho_h$  = horizontal steel reinforcement ratio
- $A$  = 1 for  $h_w/l_w \leq 0.5$ ; 0 for  $h_w/l_w > 1.0$ ; and varies linearly in between

$B$  = 0 for  $h_w/l_w \leq 0.5$ ; 1 for  $h_w/l_w > 1.0$ ; and varies linearly in between

The combination of the Barda equation for concrete (Equation 10) and the expression for steel (Equation 11) is referred to in this paper as the *Barda et al. Method*.

It should be noted that when the horizontal and vertical reinforcement ratios are the same, the reinforcement contribution to the shear capacity given by the Barda et al. method (Equation 11) becomes the same as the ACI code requirement given in Equation 4 and the Barda method given by Equation 9.

ASCE/SEI 43-05 is a recently published standard that provides performance-based and risk-consistent seismic design criteria for structures, systems, and components (SSC) in nuclear facilities. This standard provides an alternate method that could be used in place of the ACI 349-01 methods for calculating the shear strength of low rise reinforced concrete shear walls. Section 4.2.3 of ASCE 43-05, "Capacity of Low Rise Concrete Shear Walls," provides the following equation to calculate the ultimate shear strength of low rise shear walls ( $h_w/l_w \leq 2.0$ ),

$$v_u = 8.3\sqrt{f'_c} - 3.4\sqrt{f'_c} \left( \frac{h_w}{l_w} - 0.5 \right) + \frac{N}{4l_w t} + \rho_{se} f_y \quad (12)$$

$$\rho_{se} = A\rho_v + B\rho_h \quad (13)$$

$$v_u < 20\sqrt{f'_c} \quad (14)$$

in which  $\rho_{se}$  is the effective steel ratio. The ASCE 43-05 shear capacity equation is almost identical to the Barda et al. method formulation. The Barda et al. method applies to walls of aspect ratio  $h_w/l_w < 1.0$ ; while the ASCE 43-05 method applies to walls of aspect ratio  $h_w/l_w \leq 2.0$ . Parameters  $A$  and  $B$  are given as follows:

$A$  = 1 for  $h_w/l_w \leq 0.5$ ; 0 for  $h_w/l_w > 1.5$ ; and varies linearly in between

$B$  = 0 for  $h_w/l_w \leq 0.5$ ; 1 for  $h_w/l_w > 1.5$ ; and varies linearly in between

Reinforcement ratios  $\rho_v$  and  $\rho_h$  in Equation 13 are required to be less than or equal to 0.01. If  $\rho_v$  or  $\rho_h$  is greater than 0.01, then  $\rho_{se}$  shall be limited to 0.01.

Using the shear capacity, the ultimate shear strength is given by:

$$V_u = v_u d t \quad (15)$$

where  $d$  is the distance from the extreme compression fiber to the center of force of all reinforcement in tension which may be determined from a strain compatibility analysis. In lieu of an analysis,  $d$  equal to  $0.6 \times l_w$  can be used.

The ASCE 43-05 methodology is very similar to the Barda et al. formulations described earlier. The differences

primarily relate to the definition of low rise shear walls ( $h_w/l_w$  less than or equal to 2.0), calculation of the  $A$  and  $B$  parameters, limitation on  $\rho_v$  and  $\rho_u$ , and a reduced distance " $d$ " to be used to calculate total shear strength from the unit shear stress  $v_u$ .

All of the JNES test specimens to be introduced in the next section have equal steel reinforcement in the horizontal and vertical directions ( $\rho_v = \rho_u = 0.012$ ). Therefore, the steel ratio  $\rho_{se}$  will equate to the same value 0.012, regardless of the differences in calculating the parameters  $A$  and  $B$ . The limitation on  $\rho_{se}$ , when  $\rho_v$  or  $\rho_u$  is greater than 0.01, still remains a difference from the prior description of the Barda et al. method. Regarding the reduced value of  $d = 0.6 \times l_w$  (rather than  $0.8 \times l_w$ ), a conservative factor of 0.6 was selected in ASCE 43-05 to account for walls that may have a low ratio of vertical reinforcement, no integral perpendicular end walls, and only a small compressive load. All of the JNES test specimens utilized in this paper have a high ratio of vertical reinforcement with integral perpendicular end walls, and significant compressive loads; therefore, for comparison with the JNES test data, it would be unreasonable to use the 0.6 factor. For these walls the factor of 0.8 will be utilized instead. Based on the above discussion, for the JNES test specimens the only difference remaining lies in the limitation on the steel ratio  $\rho_{se}$ , which for the ASCE 43-05 method, reduces the value from 0.012 to 0.01.

## RELEVANT JNES/NUPEC SHEAR WALL TESTS

JNES/NUPEC conducted tests of 11 box type shear walls that were subjected to uni- and multi-directional cyclic loadings [8, 9]. Figure 1 shows a typical box type shear wall specimen. Among the 11 specimens, 8 box type shear walls were tested using uni-directional loadings at angles  $0^\circ$ ,  $26.6^\circ$ , and  $45^\circ$ , and 3 walls were tested using multi-directional loadings that include rectangular, cross, and diagonal cross loading scenarios, as shown in Figure 2. As shown in the first column of Table 1, the specimen ID "SD-NS-ND" series represent the specimens subjected to the uni-directional loading with NS as the shear span ratio ( $M/Qd$ ) and ND as the loading angle (degrees), while the specimens in the "SB-B-NN" series are the ones subjected to multi-directional loading with NN equal to 1, 2 and 3 as the indicator for rectangular loading, cross loading, and diagonal cross loading respectively. The shear span ratio for the "SB-B-NN" series is 0.8.

The information for these tests that is pertinent to the use of the simplified methods is presented in Table 1, in which the specimens are ordered based on their shear span ratio. The specimens presented in the first three rows have a shear span ratio of 0.6, the ones in the shaded six rows in the middle have a shear span ratio of 0.8, and the ones in the last two rows have a shear span ratio of 1.0. All specimens have the same dimensions in plan view, which is a square with each side having a length of 1.5 m (center to center distance between two flange walls). The shear walls in both directions for all 11

specimens have a thickness of 75 mm. The heights of the walls for the 3 shear span ratios are 0.7 m, 1 m, 1.3 m respectively, which results in aspect ratios of 0.47, 0.67, and 0.87 respectively. The loading slab on the top of the shear walls has a thickness of 400 mm for all 11 specimens, and the displacement-controlled loading is applied at the mid height of the loading slab. The specimens are fixed to the base slab in the tests.

Also listed in Table 1 are the uniaxial compressive strength  $f'_c$  of the concrete and the yield strength  $f_y$  of the rebars. The maximum shear strength of the walls in either horizontal direction obtained from the tests is designated as  $V_{MT}$  (strength of 2 walls in parallel) and is tabulated in this table, as well as the maximum (resultant) vector shear strength  $V_{VT}$  of the box type walls. The starred  $V_{MT}$  values in Table 1 are calculated using the maximum vector shear strength and the loading angle. It is important to observe that both  $V_{MT}$  and  $V_{VT}$  represent the same maximum loading that the test specimen can take.

All 11 shear wall specimens have double layer reinforcement of 6 mm diameter rebars at 70 mm spacing in both horizontal and vertical directions, which result in a reinforcement ratio of 1.2% for both directions. Vertical compressive loads were applied in all tests to simulate an equivalent constant axial stress of 1.47 MPa at the top of the wall, a typical value for the lower story of NPP structures in Japan.

The subsections that follow utilize the above test specimen properties to calculate the shear wall capacities of the box type structures using the ASCE 43-05 method and the ACI 349-01 methods. The lengths of the walls  $l_w$  all correspond to the same center-to-center dimension 1.5 m. Also, the two walls in parallel are considered as one wall with the thickness doubled.

## APPLICATION OF ASCE 43-05 METHOD

### Ultimate Shear Strength Comparison

Following the same order of specimens listed in Table 1, Table 2 shows the results for all 11 cases using the ASCE 43-05 method.  $V_U$  is the ultimate shear strength calculated using the ASCE 43-05 method. The data listed in columns labeled  $V_U/V_{VT}$  and  $V_U/V_{MT}$  are the ratios of the calculated ultimate shear strength to the resultant maximum vector shear strength and the same calculated ultimate shear strength to the maximum shear strength from the tests. Also listed in Table 2, the magnitude of  $V_{VT}/V_{MT}$  indicates the significance of the (concurrent) bi-axis shear force effect at the time of failure of the specimens. For example,  $V_{VT}/V_{MT} = 1$  for specimen SD-06-00 indicates that there are no concurrent bi-axis shear forces; while  $V_{VT}/V_{MT} = 1.414$  for specimen SD-06-45 shows that the bi-axial shear forces achieve their maximum at the same time. The ratio of  $V_{VT}/V_{MT}$  is therefore referred to as the *interaction intensity* in this paper. The aspect ratio of the walls, an

important factor used later in this subsection, is also listed in Table 2.

Several observations can be made based on the ratios in Table 2. By examining  $V_U/V_{MT}$ , where a value greater than one means over-prediction by the ASCE 43-05 method, there appears to be two factors that may affect the accuracy of this method. The first factor is the aspect ratio.  $V_U/V_{MT}$  is between 0.82 and 1.09 for an aspect ratio of 0.47, between 0.92 and 1.20 for an aspect ratio of 0.67, and between 1.09 and 1.41 for an aspect ratio of 0.87. In particular, when the interaction intensity is minimal, i.e.,  $V_{VT}/V_{MT} = 1$ ,  $V_U/V_{MT}$  increases from 0.82 to 1.09 as the aspect ratio increases. The data suggests that as the aspect ratio increases, the ASCE 43-05 method tends to over predict the shear strength to some extent. This observation is also consistent with the trend shown in Figure C4-1 of the ASCE 43-05 standard. The second factor is the bi-axial shear force effect (interaction intensity). For any given aspect ratio, as the interaction intensity ( $V_{VT}/V_{MT}$ ) increases, the ASCE method tends to over predict the shear strength.

As shown in Table 2, the ratios of  $V_U/V_{VT}$  are smaller than one except for the case of specimen SD-10-00 where no bi-axial shear force effect is present.  $V_U/V_{VT}$  generally increases as the aspect ratio increases: between 0.76 and 0.82 for an aspect ratio of 0.47, between 0.85 and 0.93 for an aspect ratio of 0.67, and between 1.0 and 1.09 for an aspect ratio of 0.87. For any given aspect ratio,  $V_U/V_{VT}$  appears to decrease slightly as the bi-axis effect increases.

These observations will be investigated analytically in the next two subsections, to assess how one could adjust the ASCE 43-05 method in order to more accurately predict the strengths in these tests. The discussion will be categorized into two approaches: one considers the strength adjustment based on a single wall and the other considers the strength adjustment based on treating the specimen (four walls) as an overall-box structure.

### Single-Wall Strength Adjustment Approach

The ASCE 43-05 method, as well as the Barda et al. method which it is based on, have been developed to calculate the shear strength of a single wall. Therefore, comparing  $V_U$  to  $V_{MT}$  for accuracy assessment appears to be a reasonable approach. However, the ratios of  $V_U/V_{MT}$  as shown in Table 2 are scattered above and below 1.0, and if taken literally, do not conclusively suggest any conservative or unconservative observation. The ASCE 43-05 method considers only the vertical load effect, leaving out moments and the out-of-plane shear force that can coexist in a shear wall. However for the tests, the in-plane shear force and the other forces did coexist at failure of the walls and the interaction between them can lead to a lower shear capacity. For the ASCE 43-05 method to be applicable to situations where multiple internal forces exist at the same time, it is important to take these interaction effects into account.

The consideration of interaction effect is simplified herein by utilizing the interaction intensity  $V_{VT}/V_{MT}$ . Figure 3 shows four regression analyses that fit the various permutations of the test data into power functions. The thick fitted curve is for all 11 cases, while the 3 thin fitted curves correspond to the 3 different aspect ratios. It is clear that the fit is not good if all 11 cases are considered at the same time, as indicated by the lower  $R^2$  value (0.59), which represents the variance reduction by the regression. However, if the influence of the aspect ratio is considered, by using the three separate curves, the regression equations achieve a very tight fit to the data. This finding from Figure 3 agrees with those observations discussed previously.

By assuming a general form of the power regression equation

$$\frac{V_U}{V_{MT}} = F \left( \frac{V_{VT}}{V_{MT}} \right)^c \quad (16)$$

where  $F$  is a linear function of the aspect ratio  $h_w/l_w$ , a least-square minimization of the predicted error in  $\frac{V_U}{V_{MT}}$  yields the following optimum regression equation,

$$\frac{V_U}{V_{MT}} = F \left( \frac{V_{VT}}{V_{MT}} \right)^{0.8} \quad (17)$$

$$F = 0.5 + 0.65 \frac{h_w}{l_w}$$

Table 3 compares  $V_U/V_{MT}$  predicted by Equation 17 with  $V_U/V_{MT}$  obtained using ASCE 43-05 for all 11 tests. The median ratio of Equation 17 over ASCE 43-05 for computing  $V_U/V_{MT}$  is 1.002. The logarithmic standard deviation  $\beta_{EQN}$  of the ASCE 43-05  $V_U/V_{MT}$  with respect to the regression equation is only 0.024. This shows that Equation 17 closely represents  $V_U/V_{MT}$  calculated using ASCE 43-05 for all 11 test cases.

Equation 17 can be explained further by examining two contributing factors: the bias of the ASCE 43-05 method for  $V_U$  for these 11 cases and the interaction effect. First, considering a scenario where the interaction does not exist, i.e.  $V_{VT}/V_{MT} = 1$ , Equation 17 is then simplified to

$$\frac{V_U}{V_{MT}} = F \quad (18)$$

In this expression,  $F$ , which is a function of  $h_w/l_w$ , indicates the degree of bias of the ASCE 43-05 method. Table 4 presents the calculated values of  $F$  over the range of aspect ratios that can be used with the ASCE 43-05 method. The shaded rows represent the range of the aspect ratios in the tests, and the non-shaded rows correspond to extrapolated values.  $F$  greater than one indicates that the ASCE 43-05 method produces an unconservative shear strength. As indicated in Table 4, for any aspect ratio greater than 0.77, the ASCE 43-05 equation becomes unconservative. In addition,

the ASCE 43-05 method might become significantly unconservative when  $h_w/l_w$  exceeds 1.0 and might be significantly conservative when  $h_w/l_w$  is less than 0.5. Since the aspect ratio of 0.9 results in less than a 10% unconservative bias, caution should be used when applying the ASCE 43-05 method for  $h_w/l_w$  ratios that exceed 0.9.

The second contributing factor in Equation 17 is the interaction effect from bi-axis shear forces, which is given by  $(V_{VT}/V_{MT})^{0.8}$ . This term was calculated for the possible range of  $V_{VT}/V_{MT}$ , and is tabulated in Table 5. The interaction effect always introduces an unconservative bias to the shear strength estimated by the ASCE 43-05 equation. However, if the  $V_{VT}/V_{MT} < 1.12$ , i.e., the interaction intensity is not significant, this bias is less than about 10% and for practical purposes could be neglected. For the purpose of simplifying the application,  $(V_{VT}/V_{MT})^{0.8}$  can be approximated as a linear function,

$$\left(\frac{V_{VT}}{V_{MT}}\right)^{0.8} \approx 0.2 + 0.8 \frac{V_{VT}}{V_{MT}} \quad (19)$$

and the error introduced is less than 1% for all possible values of  $V_{VT}/V_{MT}$ .

Although the interaction effect is unconservative, its combination with the  $F$  factor may lead to a larger range of applicable scenarios, especially for shear walls in nuclear power plants that typically have an aspect ratio less than 1.0. Figure 4 shows a series of  $V_U/V_{MT}$  contour curves on the  $V_{VT}/V_{MT} - h_w/l_w$  plane, where any point below the curve " $V_U/V_{MT}=1$ " indicates a conservative case for the ASCE 43-05 method. For example, when the aspect ratio is 0.5, the ASCE 43-05 method can still predict a conservative shear capacity for any interaction intensity  $V_{VT}/V_{MT} < 1.27$ , rather than the criteria  $V_{VT}/V_{MT} < 1.12$  discussed above. It also confirms that for any aspect ratio greater than 0.77, the ASCE 43-05 equation may become unconservative in spite of the interaction effect. Figure 5 shows the same contour curves in terms of the loading angle, which is defined as the angle between the wall and the resultant vector shear force, and has a maximum value of 45°. For the same wall, having an aspect ratio of 0.5, the loading angle can be as high as 38° for the ASCE 43-05 method to still predict conservative results. These figures also show that for walls with an aspect ratio less than 0.4, the interaction effect can be neglected (presuming that Equation 17 still holds beyond the aspect ratio range of [0.47, 0.87]).

### Overall-Box Strength Adjustment Approach

In assessing the effect of bi-axis shear loading, Hiroshi, et al. [9] normalized the maximum vector shear forces by the one directional shear strength calculated using a Japanese concrete design standard, and plotted the normalized maximum vector shear forces on the X-Y plane. This plot included the data for 6 box type specimens which have an aspect ratio of 0.67 and one cylindrical type specimen. This plot shows that the

maximum vector forces for these 6 box type specimens fall outside a unit circle. This trend has also been observed previously in this report using Table 2. A similar approach, with the shear strength calculated using the ASCE 43-05 method, is developed below in order to examine the interaction effect considering the overall-box structure.

Let  $V_X$  and  $V_Y$  denote the shear forces at failure in the X and Y directions from the tests, respectively, and  $V_U$  be the shear strength of two parallel walls calculated using the ASCE 43-05 method. Then, the unit circle, defined similarly to that by Hiroshi [9], can be expressed as

$$\left(\frac{V_X}{V_U}\right)^2 + \left(\frac{V_Y}{V_U}\right)^2 = 1 \quad (20)$$

or,

$$\frac{V_{VT}}{V_U} = 1 \quad (21)$$

Figure 6 shows the normalized shear forces in the X-Y plot, where all of the data conservatively fall outside the unit circle defined by Equation 20, with one exception corresponding to the SD-10-00 specimen. In another words, the ASCE 43-05 method conservatively predicts the resultant vector for all specimens except for one case if the design had been done in terms of the overall structure.

Equation 17 can be transformed into the following equation,

$$\left(\frac{V_{VT}}{V_U/F}\right) = \left(\frac{V_{VT}}{V_{MT}}\right)^{0.20} \quad (22)$$

where the right hand side represents any bias that the interaction intensity  $V_{VT}/V_{MT}$  may introduce to Equation 21, and  $V_U/F$  is the shear strength by the ASCE 43-05 method, adjusted to account for the aspect ratio. The bias term  $(V_{VT}/V_{MT})^{0.2}$  and its approximate linear form have been tabulated in Table 6. It is obvious then that the conservative bias introduced by the interaction is only 7.2% as a maximum value. Figure 7 shows the maximum vector shear forces that are normalized by  $V_U/F$ , and also demonstrates that a bias (deviation from the unit circle) grows slightly in the conservative direction as the interaction intensity  $V_{VT}/V_{MT}$  increases. This figure also exhibits much smaller variation in the normalized vector shear forces than those in Figure 6.

In this approach, the bi-axis shear force effect is directly accounted for by Equation 21. Therefore, after the bias introduced by the ASCE 43-05 method (factor  $F$ ) has been removed, the test results are very close to the unit circle with just a small additional bias.

### Discussions on Application of ASCE 43-05 Method

For shear walls with small or no interaction effects in the loading, the use of the ASCE 43-05 method has been shown to be very close and in most cases conservative when compared



to the JNES/NUPEC test results based on walls having aspect ratios in the range of 0.47 to 0.87. For walls with more significant interaction effects, and to improve the accuracy of predicting shear wall strengths for walls with small and no interaction effects, an adjustment should be applied to the ASCE 43-05 method.

In both the single-wall approach and the overall-box approach, the bi-axial effect is considered in a simplified fashion using the interaction intensity  $V_{VT}/V_{MT}$ . For general nuclear power plant structures that usually do not resemble the test specimens in terms of equal shear strengths in the two horizontal directions, symmetric wall configurations, and other aspects, these simplified approaches may not necessarily be applicable.

To enhance the accuracy of the ASCE 43-05 method, an adjustment factor should be applied. This adjustment factor can be represented very well by a linear function of the aspect ratio. In addition, application of the ASCE 43-05 method should be cautioned for shear walls having an aspect ratio greater than 0.9.

With the adjustment to the ASCE 43-05 method, both approaches can accurately account for the bi-axial effect. The apparent high level of conservatism in  $V_U/V_{VT}$  can be removed by taking out the bias from the ASCE 43-05 method. The conservative bias introduced by the interaction effect is considered small.

Generally, the interaction should be dealt with in an analytical way, rather than simply addressing it in terms of the level of conservatism or unconservatism. However, for certain ranges of shear walls (in terms of aspect ratio) and certain loading conditions, the interaction effect may be negligible. For very small aspect ratios, the interaction effect can even be totally neglected no matter how severe it is.

In the case of nuclear power plant design, the common practice is to demonstrate that the three seismic input motions are statistically independent from one another. When the seismic loads in both horizontal directions are statistically uncorrelated, the shear forces  $V_X$  and  $V_Y$  can be combined probabilistically in accordance with the 100-40-40 rule:

$$V_{VT} = \sqrt{(V_1)^2 + (0.4V_2)^2}, \quad (23)$$

where  $V_1$  (also  $V_{MT}$ ) is the larger of  $V_X$  or  $V_Y$ , and  $V_2$  is the lesser value. The maximum interaction intensity  $V_{VT}/V_{MT}$  is only:

$$\frac{V_{VT}}{V_{MT}} = \sqrt{1^2 + 0.4^2} = 1.077, \quad (24)$$

which corresponds to a loading angle of 21.8°. The unconservatism from the interaction effect is only 6.1% ( $(1.077)^{0.8} = 1.061$  from Equation 19). Thus, no significant unconservative bias is introduced by considering each

direction independently so long as the bi-axis shear components are uncorrelated.

## APPLICATION OF ACI 349-01 METHODS

Ultimate shear strengths of the 11 test specimens were calculated using the ACI 349-01 Chapter 11 and 21 methods and compared to the test results in two ways: (1) comparing the maximum shear of the two test directions and (2) comparing the maximum resultant vector shear of the bi-axis shears. A regression analysis was not performed for these two methods because it is understood that ACI 349-01 methods were developed with inherent conservatism for design purposes and a regression analysis would not yield much useful insights.

### ACI 349-01 Chapter 11 Method

Table 7 presents the predicted (calculated) shear wall strengths,  $V_U$ , for the 11 specimens using the ACI 349-01 Chapter 11 method. The calculation of the shear strength for all 11 cases is governed by the upper bound limit of  $10td\sqrt{f'_c}$ , as defined by Equation 5. The tabulated data in the columns labeled  $V_U/V_{VT}$  and  $V_U/V_{MT}$ , in Table 7, are the ratios of the predicted shear capacity to the (resultant) vector test result and to the maximum test result in both directions. Reviewing the ratios  $V_U/V_{VT}$  and  $V_U/V_{MT}$  indicates that the ACI 349-01 Chapter 11 method is conservative for all cases. The level of conservatism is very large for smaller aspect ratios and diminishes as the aspect ratio increases to 0.87.

### ACI 349-01 Chapter 21 Method

Table 8 presents the predicted shear wall strengths for the 11 specimens using the ACI 349-01 Chapter 21 method. The calculation of the shear strength for all 11 cases is also governed by the upper bound limit of  $10A_{sp}\sqrt{f'_c}$ , which is higher than the  $10td\sqrt{f'_c}$  used in the ACI 349-01 Chapter 11 method. The ratios of  $V_U/V_{VT}$  and  $V_U/V_{MT}$  show that this method is also conservative for all cases except for SD-10-45. The level of conservatism is large for smaller aspect ratios and diminishes as the aspect ratio increases. In the case of SD-10-00, which corresponds to the loading in the plane of the wall, the approach is still somewhat conservative. However, when the interaction effect is present in the test (i.e., specimen SD-10-45 with a 45° loading angle), the ratio of  $V_U/V_{MT}$  is greater than one indicating that the predicted strength is unconservative. If the interaction effect is directly considered as in the  $V_U/V_{VT}$  term, it results in a conservatively predicted value. The interaction intensity  $V_{VT}/V_{MT}$  for specimen SD-10-45 is at its maximum value of 1.414, which is however unlikely to be practical in a typical seismic design setting. As discussed previously, if the seismic loads are combined probabilistically in accordance with the 100-40-40 rule, the interaction intensity is limited to only 1.077. This level of interaction would not be likely to introduce a significant unconservative bias to the predicted shear strength for this specimen.

Both ACI 349-01 methods appear to be quite conservative for walls with low aspect ratios (i.e., less than about 0.9), which is consistent with the data shown in Figure C4-1 of the ASCE 43-05 standard.

It should be noted that the above results using the ACI 349-01 Chapter 11 and 21 methods are based on the JNES/NUPEC test specimens and so caution should be exercised in extrapolating the conclusions to other configurations/designs.

## CONCLUSIONS

The JNES/NUPEC test results from 11 box-type reinforced concrete shear wall specimens were used for assessing the ultimate shear strength estimated by simplified methods that are commonly used or intended for use in the nuclear industry. The tests included various uni-directional and multi-axial cyclic loads. These shear wall specimens have aspect ratios in the range of 0.47 – 0.87. These test data offer a valuable opportunity to assess the adequacy of simplified methods that have been mostly validated using results of single-element shear wall tests. The simplified methods considered in this paper are two methods in Chapters 11 and 21 of ACI 349-01, and one from ASCE 43-05.

For the ACI 349-01 methods, the computed ultimate shear strengths were compared against the test results in terms of the maximum shear of the two directions and the resultant of the bi-axis shears. As expected, the comparison showed that the ACI 349-01 methods appear to be quite conservative. The level of conservatism is large for smaller aspect ratios and reduces as the aspect ratio increases. In addition, the interaction intensity which measures bi-axial interaction effect also reduces the conservative margin. No significant un-conservative bias is introduced when the bi-axial seismic loads are combined by the 100-40-40 rule.

For the ASCE 43-05 method, a regression equation involving the interaction intensity and an adjustment factor  $F$  was established to closely correlate the calculated shear strength to the test data. The adjustment factor  $F$  was determined to be a linear function of the aspect ratio. For shear walls with small or no interaction effect, this method predicts conservative shear strength for walls of aspect ratios less than 0.77, and over-predicts the shear strength for walls of higher aspect ratios. Direct application of this method should be cautioned for shear walls having an aspect ratio greater than 0.9 as the unconservatism can be significant. The ASCE 43-05 method can be made very accurate by applying the adjustment factor  $F$ , provided that the regression equation is still valid beyond the aspect ratio range of 0.47 – 0.87 for the JNES/NUPEC test specimens. The interaction effect adversely affects the conservatism of this method. For walls with large interaction effect, the shear strength calculated using this method can be very close to the test data if the interaction effect is treated appropriately using the two approaches

discussed in the paper in addition to the application of the adjustment factor  $F$ .

When the two horizontal components of a seismic input motion are statistically independent of each other, the interaction effect could be neglected in application of the ASCE 43-05 method if the seismic shear forces are combined using the 100-40-40 rule. In this case, the unconservatism by neglecting the interaction effect is only 6.1%. Thus, no significant un-conservative bias is introduced by considering each direction independently so long as the bi-axis shear components are uncorrelated.

## ACKNOWLEDGEMENT

Dr. Robert P. Kennedy of RPK Structural Consulting, Inc. provided invaluable guidance for and review of the research report leading to this paper. The authors gratefully acknowledge his technical assistance and recommendations.

This work was performed under the auspices of the U.S. Nuclear Regulatory Commission, Washington, D.C., which is gratefully acknowledged.

## REFERENCES

1. ACI 349-01, "Code Requirements for Nuclear Safety Related Concrete Structures," American Concrete Institute, Farmington Hills, Michigan.
2. ASCE/SEI 43-05 (2005), "Seismic Design Criteria for Structures, Systems, and Components in Nuclear Facilities," American Society of Civil Engineers and Structural Engineering Institute.
3. Barda F., Hanson, J. M., and Corley, W. G. (1976), "Shear Strength of Low-Rise Walls with Boundary Elements," ACI Symposium, Reinforced Concrete Structures in Seismic Zones, SP-53, Detroit, Michigan.
4. Cover, L. E., Bohn, M. P., Campbell, R. D., and Wesley, D. A. (1985), "Handbook of Nuclear Power Plant Seismic Fragilities," NUREG/CR-3558, Seismic Margins Research Program, Lawrence Livermore National Laboratory.
5. Shiga, T., Shibata, A., and Tabahasi, J. (1973), "Experimental Study on Dynamic Properties of Reinforced Concrete Shear Walls," Proceedings, 5th World Conference on Earthquake Engineering, International Association for Earthquake Engineering, Rome.
6. Cardenas, A. E., Hanson, J. M., Corley, W. G., and Hognestad, E. (1973), "Design Provisions for Shear Walls," ACI Journal, Proceedings, Vol. 70, No. 3, pp. 221-230, March.

7. Oosterle, R. G., et. al. (1979), "Earthquake Resistant Structural Walls: Tests of Isolated Walls, Phase II," Construction Technology Laboratories (Division of PCA), Skokie, Illinois.
8. Habasaki, A., Kitada, Y., Nishikawa, T., Takiguchi, K., and Torita, H. (2000), "Multi-Directional Loading Test for RC Seismic Shear Walls," 12th World Conference on Earthquake Engineering (WCEE), Auckland, New Zealand.
9. Hiroshi, T., Yoshio, K., Takao, N., Katsuki, T., Hideyoshi, W., and Takeyoshi, K. (2001), "Multi-Axis Loading Test on RC Shear Walls, Overview and Outline of Two Directional Horizontal Loading Test," Transactions, SMIRT 16, Washington DC.

**TABLE 1 SPECIMEN PROPERTIES AND SHEAR STRENGTHS**

Specimen	$f'_c$ (MPa)	$f_y$ (MPa)	$h_w$ (m)	$h_w/l_w$	$V_{MT}$ (kN)	$V_{VT}$ (kN)
SD-06-00	30.7	345	0.7	0.47	1686	1686
SD-06-26	29.2	345	0.7	0.47	*1604.11	1794
SD-06-45	33.2	345	0.7	0.47	*1297.54	1835
SD-08-00	34.9	345	1	0.67	1480	1480
SD-08-26	34.8	345	1	0.67	*1401.14	1567
SD-08-45	37.4	345	1	0.67	*1161.07	1642
SB-B-01	41.3	375	1	0.67	1381	1600
SB-B-02	39.7	375	1	0.67	1596	1596
SB-B-03	34.9	375	1	0.67	1261	1588
SD-10-00	37.8	345	1.3	0.87	1231	1231
SD-10-45	37.2	345	1.3	0.87	*943.28	1334

\* calculated from  $V_{VT}$

**TABLE 2 SUMMARY OF RESULTS USING ASCE 43-05 METHOD**

Specimen	$h_w/l_w$	$V_U$ (kN)	$V_U/V_{VT}$	$V_U/V_{MT}$	$V_{VT}/V_{MT}$
SD-06-00	0.47	1383.89	0.821	0.821	1
SD-06-26	0.47	1366.65	0.762	0.852	1.118
SD-06-45	0.47	1411.70	0.769	1.088	1.414
SD-08-00	0.67	1369.98	0.926	0.926	1
SD-08-26	0.67	1369.00	0.874	0.977	1.118
SD-08-45	0.67	1394.01	0.849	1.201	1.414
SB-B-01	0.67	1483.95	0.928	1.075	1.159
SB-B-02	0.67	1469.42	0.921	0.921	1
SB-B-03	0.67	1423.98	0.897	1.129	1.259
SD-10-00	0.87	1335.30	1.085	1.085	1
SD-10-45	0.87	1330.13	0.997	1.410	1.414

**TABLE 3 COMPARISON OF PREDICTION EQUATION TO TEST RESULTS**

Specimen	ASCE 43-05 $V_U/V_{MT}$	Eq. 17 $V_U/V_{MT}$	Ratio Eq. 17 / ASCE 43-05
SD-06-00	0.821	0.804	0.979
SD-06-26	0.852	0.879	1.031
SD-06-45	1.088	1.060	0.975
SD-08-00	0.926	0.934	1.008
SD-08-26	0.977	1.021	1.045
SD-08-45	1.201	1.232	1.026
SB-B-01	1.075	1.050	0.977
SB-B-02	0.921	0.934	1.014
SB-B-03	1.129	1.123	0.994
SD-10-00	1.085	1.064	0.981
SD-10-45	1.410	1.403	0.995

Median Ratio = 1.002,  $\beta_{EQN}=0.024$

**TABLE 4 VALUES OF F**

$h_w/l_w$	F
0.35	0.728
0.47	0.806
0.50	0.825
0.67	0.936
0.77	1.001
0.87	1.066
0.90	1.085
1.00	1.150
1.50	1.475
2.00	1.800

**TABLE 5 INTERACTION EFFECT IN EQ. 17**

$V_{VT}/V_{MT}$	$(V_{VT}/V_{MT})^{0.8}$	$0.2+0.8 V_{VT}/V_{MT}$
1.000	1.000	1.000
1.077	1.061	1.062
1.120	1.095	1.096
1.159	1.125	1.127
1.259	1.202	1.207
1.414	1.319	1.331

**TABLE 6 INTERACTION EFFECT IN EQ. 22**

$V_{VT}/V_{MT}$	$(V_{VT}/V_{MT})^{0.2}$	$0.8+0.2 V_{VT}/V_{MT}$
1.000	1.000	1.000
1.077	1.015	1.015
1.120	1.023	1.024
1.159	1.030	1.032
1.259	1.047	1.052
1.414	1.072	1.083

**TABLE 7 SUMMARY OF RESULTS USING  
ACI 349-01 CHAPTER 11 METHOD**

Specimen	$h_w/l_w$	$V_U$ (kN)	$V_U/V_{VT}$	$V_U/V_{MT}$
SD-06-00	0.47	828.14	0.491	0.491
SD-06-26	0.47	807.65	0.450	0.504
SD-06-45	0.47	861.19	0.469	0.664
SD-08-00	0.67	882.97	0.597	0.597
SD-08-26	0.67	881.70	0.563	0.629
SD-08-45	0.67	914.05	0.557	0.787
SB-B-01	0.67	960.52	0.600	0.696
SB-B-02	0.67	941.73	0.590	0.590
SB-B-03	0.67	882.97	0.556	0.700
SD-10-00	0.87	918.92	0.747	0.747
SD-10-45	0.87	911.60	0.683	0.966

**TABLE 8 SUMMARY OF RESULTS USING  
ACI 349-01 CHAPTER 21 METHOD**

Specimen	$h_w/l_w$	$V_U$ (kN)	$V_U/V_{VT}$	$V_U/V_{MT}$
SD-06-00	0.47	1035.17	0.614	0.614
SD-06-26	0.47	1009.56	0.563	0.629
SD-06-45	0.47	1076.49	0.587	0.830
SD-08-00	0.67	1103.71	0.746	0.746
SD-08-26	0.67	1102.13	0.703	0.787
SD-08-45	0.67	1142.56	0.696	0.984
SB-B-01	0.67	1200.65	0.750	0.869
SB-B-02	0.67	1077.16	0.738	0.738
SB-B-03	0.67	1103.71	0.695	0.875
SD-10-00	0.87	1148.65	0.933	0.933
SD-10-45	0.87	1139.50	0.854	1.208

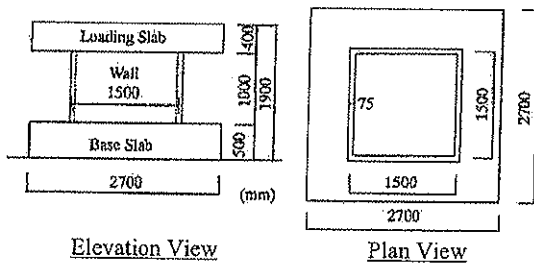


**FIGURE 1 A TYPICAL BOX TYPE SHEAR WALL  
SPECIMEN**

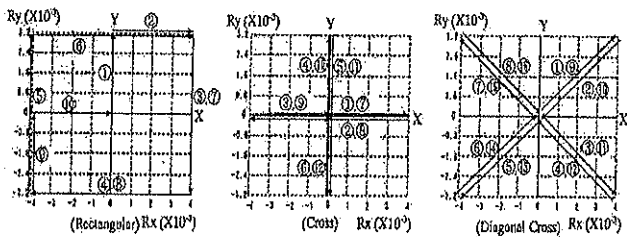


**FIGURE 2 RECTANGULAR, CROSS, AND DIAGONAL  
CROSS LOADING PATTERNS**

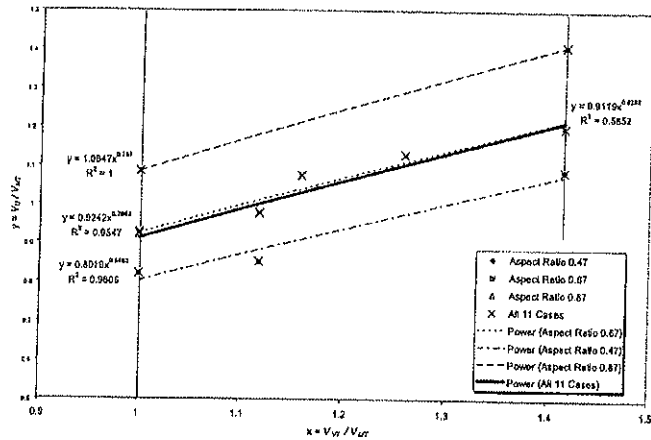


**FIGURE 3 REGRESSION ANALYSIS OF  
 $V_U/V_{MT}$  VS.  $V_{VT}/V_{MT}$**

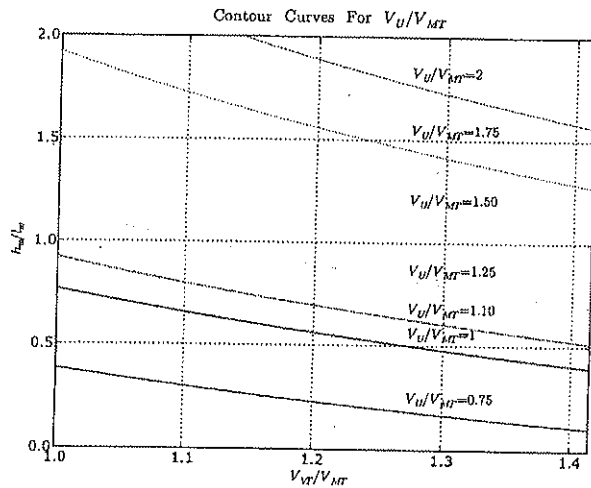


**FIGURE 4 CONTOUR PLOT OF EQ. 17**

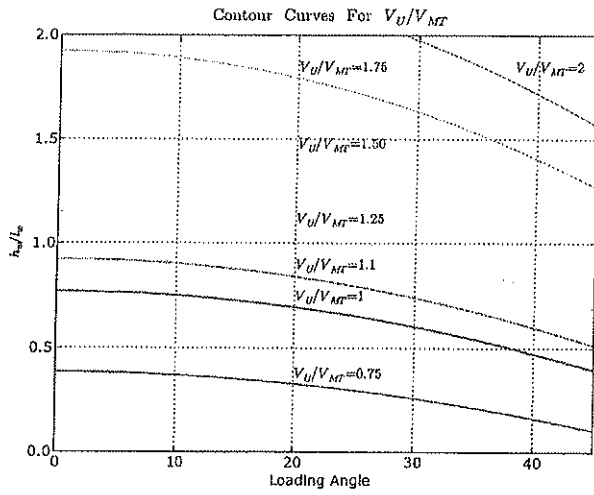


FIGURE 5 CONTOUR PLOT OF EQ. 17 IN TERMS OF LOADING ANGLE

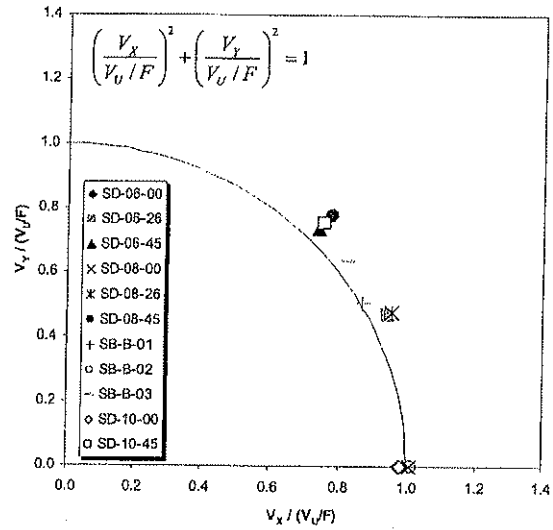


FIGURE 7 MAXIMUM VECTOR SHEAR FORCES NORMALIZED BY  $V_U/F$

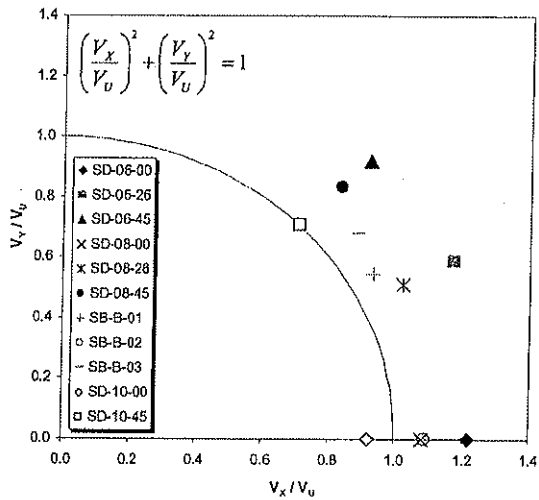


FIGURE 6 MAXIMUM VECTOR SHEAR FORCES NORMALIZED BY  $V_U$